Proceedings of the 2016 IEEE
International Conference on Robotics and Biomimetics
Qingdao, China, December 3-7, 2016

Robust Iterative Multi-Task Control of the Underwater Biomimetic Vehicle-Manipulator System

Chong Tang, Yu Wang*, Shuo Wang, and Min Tan

Abstract— **This paper presents an effective approach for multi-task control of the underwater biomimetic vehicle-manipulator system. The main idea of this approach lies in organizing and combining the tasks by priorities, while decomposes the coupled relations among the tasks by null-space mapping consecutively avoiding interaction effects. A direct kinematic model is firstly built to describe the motions and states of the end grasper. Then, the robust closed-loop iterative task-priority algorithm is designed. Here, the kinematic singularity and algorithm singularity are modified by the effective methods to ensure the robustness of the algorithm. Eventually, this algorithm is applied to solve the multi-task control problem of the underwater biomimetic vehicle-manipulator system in the grasping mission. Three noteworthy characteristics are discussed dialectically, and the obtained results show the effectiveness of this algorithm.**

I. Introduction

Cooperative manipulation and transportation of underwater vehicle in unstructured floating underwater conditions have received an increasing attention by engineers and scientists in last dozen years, which is vital to the application of underwater archaeology, oceanography and offshore industries. Tremendous efforts have been devoted to the research of underwater vehicles, which are classified into several main categories, including Human Occupied Vehicle(HOV), Remotely Operated Vehicle(ROV), and Autonomous Underwater Vehicle(AUV). And now the key is to focus on the Underwater Vehicle-Manipulator System(UVMS), which can interact with the environment so as to perform certain missions.

With our best knowledge, in underwater unstructured environment full of disturbances and uncertainties, there exits considerable challenges to accomplish the cooperative control of the vehicle body and manipulator stably, accurately and fast. Remarkably, the UVMS is nonlinear, coupled and high-dimensional systems. Generally speaking, the UVMS is usually kinematically redundant due to the degrees of freedom provided by the UVMS itself for multiple interventions effectively and flexibly. The analytical solution of the redundant system is not unique. Theoretically, the number of solutions is infinite. So on one hand, the control problem of redundant systems is hard to solve. On the other hand, multiple tasks could be executed simultaneously and accomplished successfully by exploiting the properties of the redundant degrees of freedom reasonably. Meanwhile, a number of constraints could be satisfied to protect system, such as avoiding singularity, keeping balanced.

Basically, a deal of efforts on redundancy resolution for multiple tasks have been devoted. Based on the generalized inverse of Jacobian for single task, Liegeois [1] developed a two-level adaptive control of the kinematics of multibody mechanisms consisting of the robot and the manipulator. Siciliano *et al.* [2] presented a general framework for managing multiple tasks in highly redundant robotic systems, but it was under the conditions of non-singularity. So Chiaverini [3] focused on the singularity problem and dealt with the occurrence of kinematic and algorithmic singularities, and developed singularity-robust task-priority redundancy resolution for double tasks. Antonelli [4] concluded four kinds of previous main works and analyzed the stability of prioritized closed-loop inverse kinematic algorithms for treble tasks. Antonelli *et al.* [5] proposed a fuzzy approach to redundancy resolution for UVMS for the problem of coordination between the vehicle and the manipulator. In recent years, these algorithms were further applied to practical projects or applications [6] [7] [8], for example the TRIDENT FP7 Project [9] [10].

This paper presents a robust iterative multi-task control approach on the underwater biomimetic-vehicle manipulator system(UBVMS). The main characters of this approach lie in robustness and iteration, that means multiple tasks can be planed and executed synchronously, and singularities can be avoided effectively. A kinematical model is built to describe the motions and states of the underwater biomimetic robot's manipulator. By virtue of the kinematical model, the end-grasper's motion and pose can be obtained easily. Additionally, the Jacobian relationships between the end-grasper's motions and configuration velocities can be derived in theory. That's the base of the approach above. The aims of this paper are summarized into two aspects. Firstly, we address particularly the singularity robustness to ensure the approach would still work effectively near singularity points. Secondly, an iterative strategy is introduced to manage multiple tasks.

The remainder of this paper is organized as follows. In Section II, the direct kinematical model of the UBVMS is derived. Section III reports the robust closed-loop iterative

This work was supported in part by the National Natural Science Foundation of China under Grants 61233014, 51175496, 61333016, in part by the National Key Technology Support Program 2015BAF01B01, in part by the Foundation for Innovative Research Groups of the National Natural Science Foundation of China under Grant 61421004, and in part by the Beijing Natural Science Foundation under Grant 3141002.

C. Tang is with the State Key Laboratory of Management and Control for Complex Systems, Institute of Automation, Chinese Academy of Sciences, Beijing 100190, China, and also with University of Chinese Academy of Sciences, Beijing, 100049, China.

Y. Wang, S. Wang, and M. Tan are with the State Key Laboratory of Management and Control for Complex Systems, Institute of Automation, Chinese Academy of Sciences, Beijing 100190, China.

(e-mail: yu.wang@ia.ac.cn)

Fig. 1. Underwater biomimetic vehicle-manipulator system-RobCutt II.

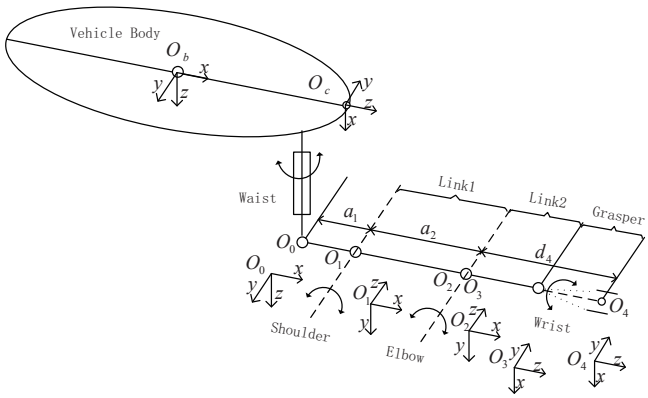

Fig. 2. Illustration of coordinate frames and notations.

multi-task control strategy. Section IV gives the results of simulations. Finally, this paper is concluded in Section V.

II. Kinematics Modeling

In this section, we first deduce the kinematical model for the UBVMS consisting of the vehicle body, two bionic drivers and a manipulator, as illustrated in Fig. 1. [11] reported the detailed mechanism and control system design of Biomimetic Underwater Vehicle(BUV) prototype propelled by two symmetrical undulating long-fins installed on both sides. Furthermore, the symmetrical undulating long-fins is redesigned and assembled modularly in RobCutt II. And a novel design of an underwater manipulator with a lightweight multilink structure was addressed in [12], which reduces the coupling between the manipulator and the vehicle efficiently.

A. Kinematical Model

For sake of clarity, the following reference frames system is adopted in this paper, as depicted in Fig. 2. Traditionally, the origin of the body-fixed frame $\sum O_b - XYZ$ coincides exactly with the center of gravity of the underwater biomimetic vehicle. In the front of the vehicle, two cameras are mounted for collecting real time images of underwater environment and sensing interesting information, and the camera frame is denoted as $\sum O_c - XYZ$, noting that the camera frame

TABLE I
D-H Parameters [12]

Link	$\theta(^\circ)$	d(mm)	a(mm)	$\alpha(^\circ)$
L_1	θ_1	0	67	90
L_2	θ_2	0	189.95	0
L_3	θ_3+90	0	0	0
L_4	θ_4	415	0	0

is located at a point decided by camera calibration, not the imaging coordinate of either of the cameras. Fig. 2 presents the initial configuration of the manipulator, where *Link1* and *Link2* are both parallel to the coronal plane of the UBVMS. The grasper is opened naturally, and the plane formed by open grasper is also parallel to the coronal plane, that means the wrist joint has no rotation. O_4 is the geometrical center of the opened grasper, so the manipulator reference frames including $\sum O_i - XYZ,\ i = 0,1,2,3,4$ are assigned. $\theta_1, \theta_2, \theta_3, \theta_4$ are corresponding waist, shoulder, elbow, wrist joint angles with respect to the frames of themselves. Additionally, earth-fixed frame (world or inertial frame) $\sum O_I - XYZ$ can be assigned flexibly according to practical requirements.

We model the manipulator as multiple links connected by joints to facilitate mathematical derivation, so the kinematical model of the underwater manipulator is easy to be built based on Denavit-Hartenberg(DH) parameters model. The specific parameters are given in Table I. For simplicity, define ${}^0T_n$ as the homogeneous matrix expressing the homogeneous transformation from the n frame to the 0 frame, n is the degree of freedom of the manipulator, here $n = 4$. So

$$ {}^0T_n = \begin{bmatrix} {}^0R_n & {}^0p_n \\ 0 & 1 \end{bmatrix} = \sum_{i=1}^{n} A_i, \tag{1} $$

where

$$ A_i = \begin{bmatrix} c_{\theta_i} & s_{\theta_i}c_{\alpha_i} & s_{\theta_i}s_{\alpha_i} & a_i c_{\theta_i} \\ s_{\theta_i} & c_{\theta_i}c_{\alpha_i} & -c_{\theta_i}s_{\alpha_i} & a_i s_{\theta_i} \\ 0 & s_{\alpha_i} & c_{\alpha_i} & d_i \\ 0 & 0 & 0 & 1 \end{bmatrix}, \tag{2} $$

c_θ, s_θ are short notations for $\cos(\theta)$ and $\sin(\theta)$ respectively.

And ${}^BT_0$, the homogeneous transformation matrix from the 0 frame to the body-fixed frame, is a constant matrix. Analogously, ${}^IT_B$, the homogeneous transformation matrix from the body-fixed frame to the earth-fixed frame, depends on the position and orientation of underwater biomimetic vehicle. By conversion rules, we can obtain

$$ {}^IT_n = {}^I T_B \, {}^B T_0 \, {}^0T_n. \tag{3} $$

Eventually, we acquired the kinematical model of the UBVMS with an explicit form in (3). With the kinematical model, we can compute the pose and motion state of the end grasper, given the joint angles. Furthermore, it will be used to derive the Jacobian relations between the system velocities and certain goals.

III. Multi-Task Control Strategy

In this section, the multi-task control algorithm is introduced from single task to multiple tasks. Additionally, the iterative process is concluded, so the algorithm can be applied to accomplish as many tasks as you need.

A. Single Task Redundancy Resolution

Define $\sigma(t) \in R^m$ as the vector of the task variable, $q(t) \in R^{6+n}$ as the configuration vector of UBVMS, including vehicle and manipulator. Obviously, the translational motion and yaw, roll rotation of the UBVMS can be driven by the double undulatory fins. While the pitch rotation is achieved by moving the inner slider along with the $O_b - X$ direction. The angle of pitch and roll are only limited to a narrow range. So $q = [x\ y\ z\ \psi\ \theta\ \phi\ \theta_1\ \theta_2\ \theta_3\ \theta_4]^T$. For simplicity, the relationship between system state q and given task σ can be formulated as

$$\sigma = f(q). \tag{4}$$

The corresponding differential relationship is

$$\dot{\sigma} = \frac{f(q)}{q}\dot{q} = J(q)\dot{q}, \tag{5}$$

where $J(q) \in R^{m\times(6+n)}$ is the Jacobian matrix and $\dot{q} \in R^{6+n}$ is the system velocity vector. Note that $m < 6+n$ in general, i.e., the $J(q)$ has more columns than rows.

Given the desired $\dot{\sigma}_d$, reference velocities of UBVMS $\dot{q}_d$ are usually generated from the inverse mapping of (5). The minimization of the task variable velocities error in weighted minimum norm sense is given as

$$S \triangleq \{\dot{q} = arg\ \underset{\dot{q}}{min}||\dot{\sigma}_d - J\dot{q}||_W^2\}. \tag{6}$$

Thus the corresponding solution is to use the generalized inverse of the Jacobian matrix [2]

$$\dot{q} = J^+\dot{\sigma}_d + [I - J^+J]z, \tag{7}$$

where $J^+ = W^{-1}J^T(JW^{-1}J^T)^{-1}$ is the weighted generalized inverse of J, which satisfies the four Moore-Penrose conditions. When W is the identity matrix, J^+reduces to basic form, i.e., $J^T(JJ^T)^{-1}$. And the first term of (7) corresponds to the minimum norm solution, while the second represents the allowed arbitrariness within the solution.

Toward to the end, the following compact notation is introduced

$$\rho_1 \triangleq J^+\dot{\sigma}_d, \tag{8}$$

$$Q_1 \triangleq [I - J^+J]. \tag{9}$$

B. Multiple Tasks Redundancy Resolution

For the UBVMS, multiple tasks can be arranged in descending priority order, hoping to satisfy all of them simultaneously. Firstly, consider a single sub-primary task. Define $\sigma_{sp1}(t) \in R^{m_{sp1}}$ as the first sub-primary task variable, the following equation holds

$$\sigma_{sp1} = f_{sp1}(q). \tag{10}$$

The differential relationship is

$$\dot{\sigma}_{sp1} = J_{sp1}\dot{q}. \tag{11}$$

The linear quadratic optimization problem

$$\dot{q} = arg\ \underset{\dot{q}}{min}||\dot{\sigma}_{sp1} - J_{sp1}\dot{q})||_W^2 \tag{12}$$

Substitute equation (7) into (12), the above optimization problem can be equivalently rewritten as

$$S_{sp1} \triangleq \{\ \dot{q} = \rho_1 + Q_1 z_{sp1} : z_{sp1} = arg\ \underset{z_{sp1}}{min}||\dot{\sigma}_{sp1} - J_{sp1}\rho_1 - J_{sp1}Q_1 z_{sp1}||_W^2\}. \tag{13}$$

Let $\hat{J}_{sp1} = J_{sp1}Q_1$, the following solution could be obtained

$$z_{sp1} = \hat{J}_{sp1}^+(\dot{\sigma}_{sp1} - J_{sp1}\rho_1) + (I - \hat{J}_{sp1}^+\hat{J}_{sp1})z_{sp2}. \tag{14}$$

And plug (14) into (7)

$$\begin{aligned}\dot{q} &= \rho_1 + Q_1(\hat{J}_{sp1}^+(\dot{\sigma}_{sp1} - J_{sp1}\rho_1) + (I - \hat{J}_{sp1}^+\hat{J}_{sp1})z_{sp2}) \\ &= (\rho_1 + Q_1\hat{J}_{sp1}^+(\dot{\sigma}_{sp1} - J_{sp1}\rho_1)) + Q_1(I - \hat{J}_{sp1}^+\hat{J}_{sp1})z_{sp2}.\end{aligned} \tag{15}$$

By observing that the null-space projection operator Q_1 owes both properties of Hermitian and idempotent, i.e., matrix satisfies $A^H = A$, $A^n = A$. [13] has proved that $Q_1\hat{J}_{sp1}^+ = \hat{J}_{sp1}^+$, so (15) can be simplified to

$$\begin{aligned}\dot{q} &= (\rho_1 + \hat{J}_{sp1}^+(\dot{\sigma}_{sp1} - J_{sp1}\rho_1)) + Q_1(I - \hat{J}_{sp1}^+\hat{J}_{sp1})z_{sp2} \\ &= \rho_{sp1} + Q_{sp1}z_{sp2}.\end{aligned} \tag{16}$$

Here, it's obvious that

$$\rho_{sp1} = [I - \hat{J}_{sp1}^+J_{sp1}]\rho_1 + \hat{J}_{sp1}^+\dot{\sigma}_{sp1}, \tag{17}$$

$$Q_{sp1} = Q_1[I - \hat{J}_{sp1}^+J_{sp1}]. \tag{18}$$

Now the iteration process is clear, and it is convenient to be expanded to all successive tasks in a descending priority order. Before formulating the iteration of task-priority algorithm, the forthcoming problems should be solved firstly.

C. Singularity-Robust Modification

In the equation (16), two kinds of singularity may occur possibly, which are kinematic singularity and algorithmic singularity respectively. Kinematic singularity is caused by motion states and mechanical structure. While algorithmic singularity is because of the algorithm's internal drawbacks.

Kinematic singularity means that the Jacobian matrix J loses full rank, which leads to JJ^T irreversible. And this reduces the feasible velocity capabilities of the end effector and results in additional possibilities of null-space velocities. So following kinematic singularity robust form[20] is adopted

$$J^+ = W^{-1}J^T(JW^{-1}J^T + p(\Sigma(JW^{-1}J^T))^{-1}, \tag{19}$$

where $p(\Sigma(JW^{-1}J^T))$ is bell-shaped function, finite support, positive matrix function parameterized by the Σ of singular value decomposition, $JW^{-1}J^T = U\Sigma V^T$, i.e., when $JW^{-1}J^T$ is close to singular, $p(\Sigma(JW^{-1}J^T))$ is used to prevent J^+ from growing to infinite.

And algorithmic singularity occurs when $\hat{J}_{sp1} = J_{sp1}Q_1$ loses rank with full-rank J_{sp1} and Q_1. When an algorithmic

singularity occurs, the execution of the sub-primary task always affects the primary task, so those two task is not compatible. Chiaverini et al. [3] analyzed the occurrence of algorithmic singularity in detail and provided an effective algorithmic singularity-robust scheme. (13) means that

$$\dot{\sigma}_{sp1} = J_{sp1}\rho_1 + J_{sp1}Q_1 z_{sp1}. \tag{20}$$

[14] pointed out that only when $\dot{\sigma}_{sp1} \in R(J_{sp1})$, the above equation can be achieved, so the following equation holds

$$J_{sp1}J_{sp1}^{+}\dot{\sigma}_{sp1} = J_{sp1}\rho_1 + J_{sp1}Q_1 z_{sp1}, \tag{21}$$

and the further simplified equation is

$$J_{sp1}^{+}\dot{\sigma}_{sp1} = \rho_1 + Q_1 z_{sp1}. \tag{22}$$

Then, the optimization problem (13) is equivalent as

$$\begin{aligned} S_{sp1} \triangleq \{ \dot{q} = \rho_1 + Q_1 z_{sp1} : z_{sp1} \\ = arg \min_{z_{sp1}} ||J_{sp1}^{+}\dot{\sigma}_{sp1} - \rho_1 - Q_1 z_{sp1}||_W^2 \}. \end{aligned} \tag{23}$$

Furthermore, according to the property of idempotent matrix and Moore-Penrose conditions, the solution is given as

$$z_{sp1} = Q_1 J_{sp1}^{+}\dot{\sigma}_{sp1} + (I - Q_1^{+}Q_1)z_{sp2}. \tag{24}$$

Substitute the above equation into (7), and the final resolution is

$$\begin{aligned} \dot{q} &= \rho_1 + Q_1(Q_1 J_{sp1}^{+}\dot{\sigma}_{sp1} + (I - Q_1^{+}Q_1)z_{sp2}) \\ &= \rho_1 + Q_1 Q_1 J_{sp1}^{+}\dot{\sigma}_{sp1} + Q_1(I - Q_1^{+}Q_1)z_{sp2} \\ &= \rho_1 + Q_1 J_{sp1}^{+}\dot{\sigma}_{sp1} \\ &\triangleq \rho_{sp1}. \end{aligned} \tag{25}$$

In (25) and (7), $\dot{\sigma}_{sp1}$ or $\dot{\sigma}_d$ are the planned desired task variable velocities. For the purpose of stronger stability, desired velocities are replaced by the combination of desired velocities and the task errors. Eventually, we formulate the robust closed-loop iterative task-priority algorithm as illustrated by Algorithm 1. This algorithm mainly works in velocity layer of the UBVMS, and the output is the desired vehicle and joint velocity of the the UBVMS, which is also the input of dynamic control module.

Algorithm 1 Closed-Loop Task-Priority Algorithm

Initialization
  $\rho_0 = 0, Q_0 = I$;
  $i = 1, z = 0$;
  $tasknum = m$;
if (*task is over*) **then**
  $\dot{q} = \rho_i + Q_i z$;
else
  Execute task plan to obtain $\dot{\sigma}_i$;
  Compute corresponding J_i;
  Compute corresponding $\tilde{\sigma}_i$;
  $Q_i = Q_{i-1}(I - J_i^{+}J_i)$;
  $\rho_i = \rho_{i-1} + Q_{i-1}J_i^{+}(k_{i1}\dot{\sigma}_i + k_{i2}\tilde{\sigma}_i)$;
  $i++$;
end if

IV. Tasks Analysis and Simulations

In this section, the robust closed-loop iterative task-priority algorithm is applied to the multi-task control of the UBVMS. Firstly, the required tasks are analyzed in the grasping mission, and corresponding Jacobian matrixes are built based on the kinematical model. Thereafter, simulations are carried out to verify the effectiveness of this algorithm.

A. Tasks Analysis

Unlike the cars with four wheels and fixed-wing airplanes, the underwater biomimetic vehicle can spin at the very same point, i.e., the tuning radius can reach to zero. So, in the perspective of minimum path and saving energy, the heading direction should be considered firstly. Thereafter, the grasper must reach the position of the target. Meanwhile, in order to grasp the target smoothly and stably, both of the desired pitch and roll angles are set to zero. Finally, the preparing grasping pose of the manipulator should be designed specially.

1) Task 1: Heading Direction: When the pitch and roll are restricted to zero, the heading direction is decided by yaw only. And the Jacobian matrix $J_1 \in R^{1\times 6+n}$ relates the system velocities $\dot{q}$ expressed in the frames of themselves with the yaw rate $\dot{\sigma}_1$ expressed in earth-fixed frame, i.e.,

$$\dot{\sigma}_1 = J_1\dot{q}, \tag{26}$$

where $J_1 = [O_{1\times 3}\ [0\ 0\ 1]J_{k,o}^{-1}\ O_{1\times n}]$, and $J_{k,o} \in R^{3\times 3}$ can be expressed in terms of Euler angles as

$$J_{k,o} = \begin{bmatrix} 1 & 0 & -s_\theta \\ 1 & c_\phi & c_\theta s_\phi \\ 0 & -s_\phi & c_\theta c_\phi \end{bmatrix}. \tag{27}$$

2) Task 2: Grasper Position: A more fine control of the end grasper may be achieved by feedback of the whole end grasper position $\sigma_2 \in R^3$ expressed in earth-fixed frame. The Jacobian matrix J_2 relates the system velocities $\dot{q}$ with the differential of end grasper position $\dot{\sigma}_2$ expressed in earth-fixed frame, as

$$\dot{\sigma}_2 = J_2\dot{q}, \tag{28}$$

where $J_2 = [{}^{I}R_B\ \ -(S({}^{I}R_B\,{}^{B}r_{B0}) + S({}^{I}R_0\,{}^{0}r_{0e}))\ J_{pos,man}]$, and $J_{pos,man}$ is manipulator position Jacobian matrix, relating the differential of end grasper position with joint angle velocities.

3) Task 3: Pitch and Roll: In analogous manner, roll and pitch can be controlled by defining $\sigma_3 = [\psi\ \theta]^T \in R^2$, and Jacobian relation is

$$\dot{\sigma}_3 = J_3\dot{q}, \tag{29}$$

where $J_3 = \begin{bmatrix} O_{2\times 3} & \begin{bmatrix} 1 & 0 & 0 \\ 0 & 1 & 0 \end{bmatrix} J_{k,o}^{-1} & O_{2\times n} \end{bmatrix}$.

4) Task 4: Manipulator Configuration: The UBVMS exhibits a pre-grasping configuration, and it is appropriate to define the task to control its position in the joint space with the simple task, $\sigma_4 = [\theta_1 \cdots \theta_n]^T \in R^n$, and the trivial Jacobian $J_4 = [O_{n\times 6}\ I_{n\times n}]$.

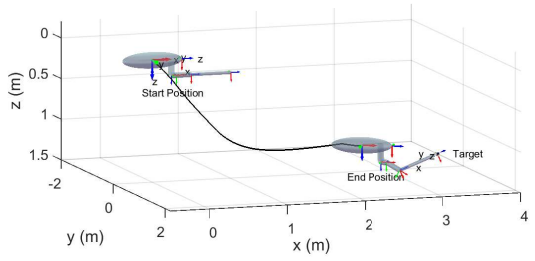

Fig. 3. Motion path and beginning-end states of UBVMS.

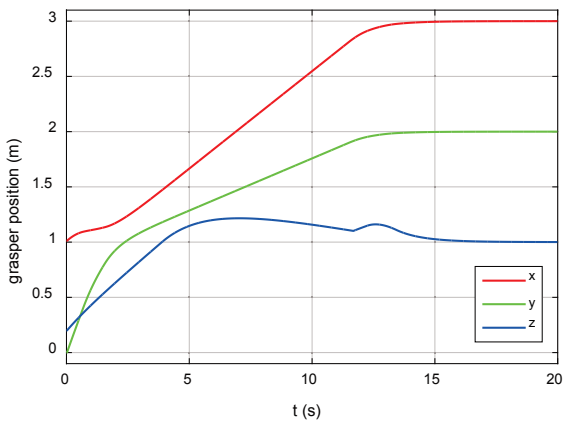

Fig. 4. End grasper position.

B. Simulations

The robust closed-loop iterative task-priority algorithm is applied to the multi-task control of the UBVMS. In the simulations, the UBVMS sets out from the origin with initial configuration. The mission is to swim stably to the position of the object at $P_{obj} = [3\ \ 2\ \ 1]^T$ and then grasp a target with certain manipulator configuration, here $\sigma_4 = [0, 45, -60, 0]^T$. The start state, end state and the motion path of the UBVMS are depicted in Fig. 3, from which, we can find that the UBVMS arrives at the target position successfully with smooth path. Fig. 4 shows the grasper's trajectories. Finally the grasper reaches to the desired point exactly. The task errors are given in Fig. 5. The primary task error soon converges to zero as shown in Fig. 5(a), that means heading direction is already adjusted properly. And the Fig. 5(b) depicts the fact again that the grasper reaches to the desired point exactly. The task 4 is assigned when the vehicle gets rather close to the target. So the errors of task 4 have a sharp change in Fig. 5(d). At last, all of them converge to zero by controlling. Fig. 6 shows system configuration information of the whole motion of the UBVMS, including the vehicle position, vehicle orientation, joint position. Comparing Fig. 6(a) and 6(b), the desired yaw

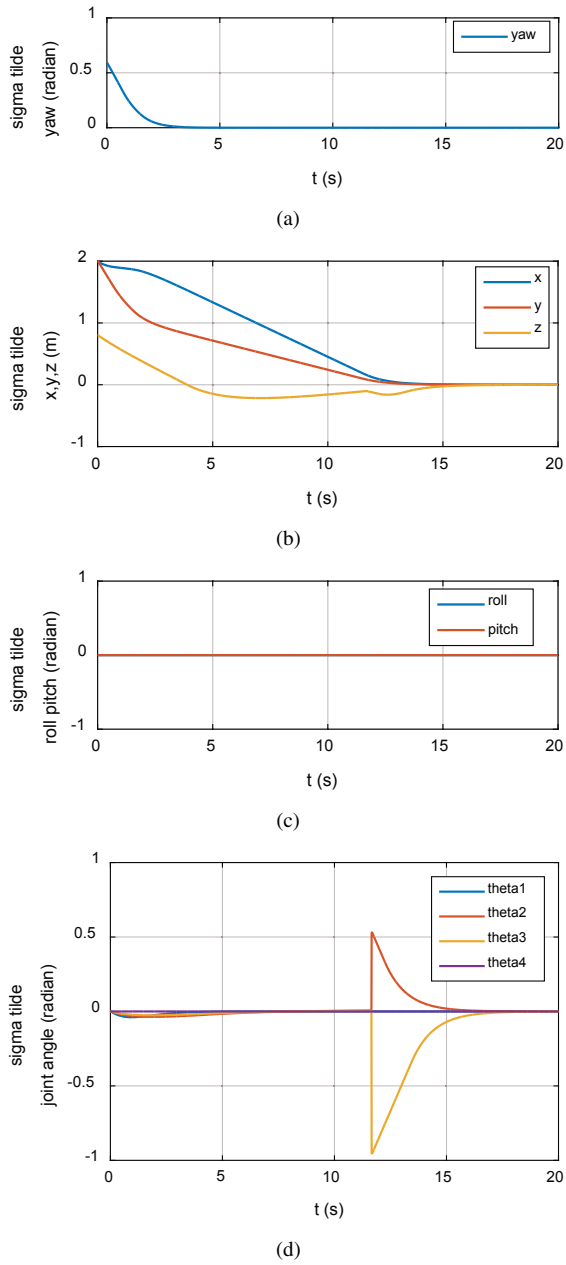

Fig. 5. Errors of Task. (a) Error of yaw. (b) Errors of end grasper position. (c) Errors of pitch and roll. (d) Errors of joint angles.

is completed firstly at about 3.5s with top priority, and the final desired position is arrived at about 15s. In addition, the pitch and roll are always zero, and the shoulder, elbow angle reach to desired states finally. So all tasks are performed successfully.

C. Discussion

Three important characteristics can be concluded from the derivation of the robust closed-loop iterative task-priority algorithm and simulations of multi-task control.

1) The robust closed-loop iterative task-priority algorithm always overcomes the drawbacks caused by the occurrences of both kinematic singularity and algorithm singularity,

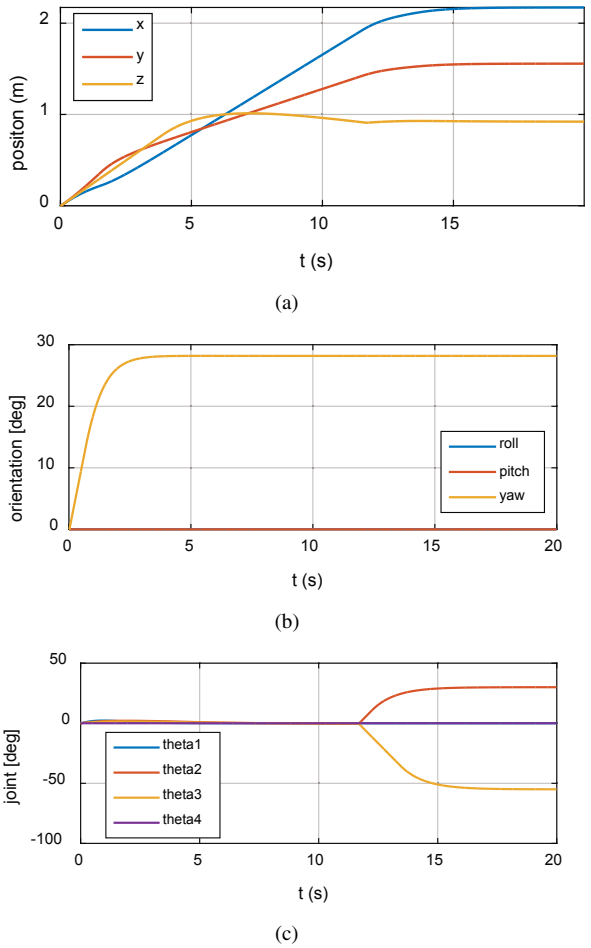

Fig. 6. System configuration of UBVMS. (a) Vehicle position. (b) Vehicle orientation. (c) Joint position.

i.e., it would still work well even though at the actual singularity points.

2) The robust closed-loop iterative task-priority algorithm is applied to the multi-task control of the UBVMS. Apparently, the tasks are designed meticulously and arranged by descending priority order according to practical requirements. Whenever the task is assigned during the process of performing missions, it can work effectively as usual, which provides marvelous flexibility and accessibility. From the simulation results, we can find that this algorithm is greatly suited to multi-task control, acquiring sound control effect.
3) In this paper's simulations, the number of control tasks is four. Actually, the number can be extended further to fit as many as missions require. However, the more tasks are, the possibility of interfering with each other is bigger, resulting in control failure or potential unknown influences.

V. Conclusions and Future Work

This paper has concentrated on the multi-task control of the UBVMS propelled by undulatory fins, whose direct kinematic model is first developed. Then, the robust closed-loop iterative task-priority algorithm is designed. Finally, the robust closed-loop iterative task-priority algorithm is applied to the mission of target grasping consisting of four basic tasks. And the simulations are conducted to verified the effectiveness of this algorithm.

In the future, we will take advantage of the robust closed-loop iterative task-priority algorithm for multi-task control and apply it into the practical control of the UBVMS in pool environment and further wild lakes environment. We will explore the possibility of improving specific control performance by optimizing the control architecture and details.

References

[1] A. Liegeois, "Automatic supervisory control of the configuration and behavior of multibody mechanisms," *IEEE Transactions on Systems, Man, and Cybernetics*, vol. 7, no. 12, pp. 868–871, Dec 1977.

[2] B. Siciliano and J. J. E. Slotine, "A general framework for managing multiple tasks in highly redundant robotic systems," in *Proceedings 5th International Conference on Advanced Robotics*, Pisa, 1991, pp. 1211–1216.

[3] S. Chiaverini, "Singularity-robust task-priority redundancy resolution for real-time kinematic control of robot manipulators," *IEEE Transactions on Robotics and Automation*, vol. 13, no. 3, pp. 398–410, Jun 1997.

[4] G. Antonelli, "Stability analysis for prioritized closed-loop inverse kinematic algorithms for redundant robotic systems," *IEEE Transactions on Robotics*, vol. 25, no. 5, pp. 985–994, 2009.

[5] G. Antonelli and S. Chiaverini, "A fuzzy approach to redundancy resolution for underwater vehicle-manipulator systems," *Control Engineering Practice*, vol. 11, no. 4, pp. 445–452, 2003.

[6] P. Cieslak, P. Ridao, and M. Giergiel, "Autonomous underwater panel operation by GIRONA500 UVMS: A practical approach to autonomous underwater manipulation," in *2015 IEEE International Conference on Robotics and Automation (ICRA)*, Seattle, Washington, 2015, pp. 529–536.

[7] E. Simetti, G. Casalino, S. Torelli, A. Sperinde, and A. Turetta, "Experimental results on task priority and dynamic programming based approach to underwater floating manipulation," in *IEEE Oceans*, Bergen, 2013, pp. 1–7.

[8] E. Simetti, G. Casalino, S. Torelli, A. Sperind, and A. Turetta, "Floating underwater manipulation: Developed control methodology and experimental validation within the trident project," *Journal of Field Robotics*, vol. 31, no. 3, pp. 364–385, 2014.

[9] D. Ribas, P. Ridao, L. Magi, N. Palomeras, and M. Carreras, "The Girona 500, a multipurpose autonomous underwater vehicle," in *IEEE Oceans*, Spain, 2011.

[10] D. Ribas, N. Palomeras, P. Ridao, M. Carreras, and A. Mallios, "Girona 500 AUV: From survey to intervention," *IEEE/ASME Transactions on Mechatronics*, vol. 17, no. 1, pp. 46–53, Feb 2012.

[11] Q. Wei, S. Wang, X. Dong, L. Shang, and M. Tan, "Design and kinetic analysis of a biomimetic underwater vehicle with two undulating longfins," *Acta Automatica Sinica*, vol. 39, no. 8, pp. 1330–1338, 2013.

[12] Y. Wang, S. Wang, Q. P. Wei, M. Tan, C. Zhou, and J. Z. Yu, "Development of an underwater manipulator and its free-floating autonomous operation," *IEEE/ASME Transactions on Mechatronics*, vol. 21, no. 2, pp. 815–824, Apr 2016.

[13] A. A. Maciejewski and C. A. Klein, "Obstacle avoidance for kinematically redundant manipulators in dynamically varying environments," *International Journal of Robotics Research*, vol. 4, no. 3, pp. 109–117, 1985.

[14] S. Chiaverini, "Task-priority redundancy resolution with robustness to algorithmic singularities," *Preprints Syroco*, vol. 94, pp. 453–459, 1994.